BJ www.biochemj.org

BJ Structure

Biochem. J. (2009) **421**, 415–423 (Printed in Great Britain) doi:10.1042/BJ20090379

Antiparallel β-sheet: a signature structure of the oligomeric amyloid β-peptide

Emilie CERF*[1], Rabia SARROUKH*[1], Shiori TAMAMIZU-KATO†, Leonid BREYDO‡, Sylvie DERCLAYE§, Yves F. DUFRÊNE§, Vasanthy NARAYANASWAMI†‖, Erik GOORMAGHTIGH*, Jean-Marie RUYSSCHAERT* and Vincent RAUSSENS*[2]

*Center for Structural Biology and Bioinformatics, Laboratory for Structure and Function of Biological Membranes, Faculté des Sciences, Université Libre de Bruxelles, CP 206/2, Blvd. du Triomphe, B-1050 Brussels, Belgium, †Center for the Prevention of Obesity, Cardiovascular Disease and Diabetes, Children's Hospital Oakland Research Institute, 5700 Martin Luther King Jr. Way, Oakland, CA 94609, U.S.A., ‡Department of Molecular Biology and Biochemistry, University of California at Irvine, 3438 McGaugh Hall, Irvine, CA 92697, U.S.A., §Unité de Chimie des Interfaces, Université Catholique de Louvain, Croix du Sud 2/18, B-1348 Louvain-la-Neuve, Belgium, and ‖Department of Chemistry and Biochemistry, California State University, Long Beach, 1250 Bellflower Boulevard, Long Beach, CA 90840, U.S.A.

AD (Alzheimer's disease) is linked to Aβ (amyloid β-peptide) misfolding. Studies demonstrate that the level of soluble Aβ oligomeric forms correlates better with the progression of the disease than the level of fibrillar forms. Conformation-dependent antibodies have been developed to detect either Aβ oligomers or fibrils, suggesting that structural differences between these forms of Aβ exist. Using conditions which yield well-defined Aβ-(1–42) oligomers or fibrils, we studied the secondary structure of these species by ATR (attenuated total reflection)–FTIR (Fourier-transform infrared) spectroscopy. Whereas fibrillar Aβ was organized in a parallel β-sheet conformation, oligomeric Aβ displayed distinct spectral features, which were attributed to an antiparallel β-sheet structure. We also noted striking similarities between Aβ oligomers spectra and those of bacterial outer membrane porins. We discuss our results in terms of a possible organization of the antiparallel β-sheets in Aβ oligomers, which may be related to reported effects of these highly toxic species in the amyloid pathogenesis associated with AD.

Key words: Alzheimer's disease, amyloid β-peptide, antiparallel β-sheet, infrared spectroscopy, oligomeric Aβ, OmpF.

INTRODUCTION

AD (Alzheimer's disease) is a widespread form of dementia and is one of a variety of amyloidoses whose common feature is the aggregation of misfolded proteins and/or peptides. AD is a brain-specific degenerative disease, neuropathologically characterized by the presence of fibrillar amyloid deposition in extraneuronal spaces/cerebrovascular regions and by neurofibrillary tangles inside the neurons [1].

Amyloid plaques are primarily composed of Aβ (amyloid β-peptide) (38–43 residues long), which is released after proteolytic cleavage of the APP (amyloid precursor protein) by β- and γ-secretases [2]. The amyloid hypothesis suggests that Aβ accumulation in the brain is the primary event in the pathogenesis. Formation of tau protein tangles could be one of the consequences of an imbalance between production and clearance of Aβ [1]. Aβ-(1–42) and Aβ-(1–40) are the principal components of amyloid plaques [3]. Aβ-(1–42) is the highly amyloidogenic, though less abundant form, which appears to be deposited initially [4]. This higher ability of Aβ-(1–42) to aggregate has been related to two additional hydrophobic amino acids at its C-terminal end [5].

Several aggregation states have been identified for amyloidogenic proteins. Aβ can exist as a monomer or larger soluble entities called oligomers and eventually insoluble fibrils. The general term 'oligomers' includes different kinds of assembly such as dimers, trimers, protofibrils, ADDLs (Aβ-derived diffusible ligands), and annular or pore-like oligomers [6]. Recently, it has also been reported that oligomers could be classified into prefibrillar or fibrillar oligomers as they have different aggregation pathways [7].

Aβ deposition in brain to form fibrillar plaques has been associated for a long time with neurodegeneration, insidious memory loss and cognitive decline [2,8]. However, there has been a paradigm shift in this concept and it is now widely accepted that soluble oligomers of Aβ are more neurotoxic than Aβ fibrils and play a direct role in the amyloid pathogenesis [9]. Cognitive decline associated with AD precedes amyloid deposition in human and transgenic mouse models and correlates with soluble Aβ oligomer levels rather than either APP levels or fibrillar amyloid deposits [10].

Aβ oligomers are most probably intermediates in amyloid fibril formation. However, they are not necessarily required to form fibrils [11]. Recently, a conformation-dependent antibody has been shown to detect amyloid fibrils with high specificity, regardless of their sequence [7]. Previously, using another conformation-dependent antibody raised against Aβ prefibrillar oligomers, it was demonstrated that many amyloidogenic proteins or peptides, which also form oligomers, were recognized by the same antibody. Therefore different types of amyloid oligomers may adopt a common structural motif postulated to be crucial in their common toxicity [12].

Obtaining any new structural information about Aβ oligomers would be an important step in better understanding of the causation of AD, and possibly other amyloidogenic diseases. Previous studies carried out on Aβ oligomers reported the dominance of β-sheet structures. However, they were unable to distinguish between parallel and antiparallel structures [5]. In the present study, we use ATR (attenuated total reflection)–FTIR (Fourier-transform infrared) spectroscopy to compare the structures of Aβ-(1–42) oligomers and fibrils. We demonstrate

Abbreviations: Aβ, amyloid-β peptide; AD, Alzheimer's disease; ADDL, Aβ-derived diffusible ligands; AFM, atomic force microscopy; APP, amyloid precursor protein; ATR, attenuated total reflection; FTIR, Fourier-transform infrared; HFIP, hexafluoropropan-2-ol; TBS, Tris-buffered saline; ThT, thioflavin T.

[1] These authors contributed equally to this work.

[2] To whom correspondence should be addressed (email vrauss@ulb.ac.be).

that, although both forms adopt a predominantly β-sheet structure, Aβ-(1–42) oligomers adopt an antiparallel β-sheet structure, which is distinctly absent from fibrils.

EXPERIMENTAL

Peptide preparation

Aβ-(1–42) was purchased from American Peptide. The peptide was dissolved in cold HFIP (hexafluropropan-2-ol; Sigma–Aldrich) at a 2 mg/ml concentration, incubated at room temperature (25 °C) for 1 h and divided into aliquots of 25 μl. HFIP was evaporated under nitrogen flow and residual HFIP was removed under vacuum using a Speed Vac (Thermo Savant). The resulting Aβ-(1–42) film was stored at − 20 °C until further manipulation.

Aβ-(1–42) incubations

Prior to any incubation, the peptide was dissolved in DMSO (Sigma–Aldrich) at a final concentration of 5 mM and then immediately resuspended using one of the following conditions. To obtain oligomers, the peptide was either dissolved in F12 Phenol Red-free cell culture medium (Sigma–Aldrich) as developed by Dahlgren et al. [13] and Stine et al. [14] or in TBS (Tris-buffered saline: 20 mM Tris/HCl, pH 7.4, 100 mM NaCl) as developed by Garzon-Rodriguez et al. [15], at a final concentration of 100 μM and incubated at 4 °C for 24 h. To obtain fibrils, the peptide was resuspended either in 10 mM HCl at a final concentration of 100 μM and incubated at 37 °C for 24 h, or in 0.5 mM Hepes, pH 7.4, at a final concentration of 500 μM and incubated at room temperature under gentle agitation for at least 30 days.

Western blot analysis

Peptide samples were diluted in SDS/PAGE sample buffer and separated on a 12 % Bis-Tris gel at 4 °C for 2 h at 100 V. The separated bands were transferred on a nitrocellulose membrane which was then blocked for 1 h in 5 % non-fat dry milk in TBS/Tween 20 buffer (10 mM Tris/HCl, pH 8, 150 mM NaCl, 0.0625 % Tween 20). The membrane was incubated with the mouse monoclonal Aβ antibody 6E10 (1:3000) (Sigma–Aldrich). Detection was carried out using horseradish peroxidase-conjugated anti-mouse antibody (1:2000) and the Supersignal West Pico Chemiluminescent Substrate (Pierce Biotechnology). Pictures were recorded and analysed using the ImageQuant 400 gel imager and ImageQuant TL software (GE Healthcare).

AFM (atomic force microscopy)

Aβ-(1–42) solutions were characterized by AFM using a Nanoscope IIIa (Veeco Metrology LLC) equipped with a 120 μm × 120 μm piezoelectric scanner. Analyses were carried out either in contact or in tapping mode at room temperature in air using AFM cantilevers with a spring constant of either 0.01 or 0.03 N/m (Microlevers, Veeco Metrology LLC). Before analysis, 100 μl of sample (diluted 10-fold in the case of fibrils and 5-fold in the case of oligomers) were incubated for 10 min at room temperature on freshly cleaved mica and rinsed four times with milliQ water. Excess water was then removed under nitrogen flow.

ThT (Thioflavin T) fluorescence

ThT (Sigma–Aldrich) fluorescence was used to characterize the different peptide solutions according to LeVine [16] on a LS55 fluorimeter (PerkinElmer Instruments). Briefly, 4.5 μg of peptide was added to 1 ml of a 5 μM ThT solution maintained at 25 °C by a circulating water bath and the fluorescence was recorded at 482 nm (excitation wavelength of 450 nm).

Dot-blot analysis

A 1 μg sample of oligomeric Aβ was spotted on a nitrocellulose membrane, which was subsequently blocked with 10 % non-fat dry milk in TBS/Tween 20 (0.01 %) for 1 h at 4 °C and washed. The membrane was then incubated overnight at 4 °C with rabbit anti-oligomer antibody A11 (1:3000) (a gift from Dr C. Glabe, University of California at Irvine, Irvine, U.S.A.) in 5 % non-fat dry milk in TBS/Tween 20 (0.01 %). After washing with TBS/Tween 20 (0.01 %), the membrane was incubated for 1 h at 4 °C with horseradish peroxidase-conjugated anti-rabbit IgG (Cell Signaling Technology) (1:2000). An ECL® (enhanced chemiluminescence) Western blot kit detection system (GE Healthcare) was used to detect chemiluminescence, and images were recorded and analysed using the ImageQuant 400 gel imager and ImageQuant TL software (GE Healthcare).

IR spectroscopy

IR spectra were recorded on an Equinox 55 infrared spectrophotometer (Bruker Optics) equipped with a Golden Gate reflectance accessory (Specac). The internal reflection element was a diamond crystal (2 mm × 2 mm) with an aperture angle of 45° that yielded a single internal reflection. 128 accumulations were performed to improve the signal/noise ratio. The spectrometer was continuously purged with dried air. Spectra were recorded at a resolution of 2 cm^{-1}. All measurements were made at 24 °C. Samples were prepared by spreading 2 μl of peptide solution on the diamond crystal surface and by removing the excess water under nitrogen flow. Alternatively, for salt-containing samples, similarly to the AFM sample preparation, 5 μl of peptide solution were incubated at the diamond surface for 15–20 min, the sample was then washed three times with excess milliQ water. Finally, excess water was removed under nitrogen flow.

H–D (Hydrogen–deuterium) exchange

H–D exchange experiments were performed on Aβ oligomers and fibrils. The pH of the samples was adjusted in order to perform the exchange on samples with identical pH. The decay of the NH-associated amide II band (1520–1580 cm^{-1}) was used to monitor the exchange of the amide group. Results were analysed as previously described [17].

Spectral cluster analysis

Before analysis, a linear baseline was subtracted from all spectra at 1708, 1602 and 1482 cm^{-1}. Spectra were then rescaled on the amide I area (1708–1602 cm^{-1}). Spectra were clustered according to the Euclidian distances for each wavenumber in the amide I and II range (1708–1482 cm^{-1}).

Protein spectra used for the clustering analysis were extracted from the RASP50 database [18]: alcohol dehydrogenase (ADH) from horse liver; α-lactalbumin (ALA) from human milk; apolipoprotein E3 (APE) from human; α-haemolysin (ATX, alphatoxin) from *Staphylococcus aureus*; avidin (AVI) from hen egg white; erabutoxin b (BTE) from *Laticauda semifasciata*; carbonic anhydrase (CAH) from bovine erythrocyte; concanavalin A (CNA) from jack bean; colicin A (COL), C-terminal domain from bacterial source; citrate synthetase (CSA) from porcine heart; α-chymotrypsinogen A (CTG) from bovine pancreas;

cytochrome *c* (CYC) from horse heart; dihydropteridine reductase (DPR) from sheep liver; apo-ferritin (FTN) from horse spleen; glutathione transferase (GST) from equine liver; haemoglobin (HBN) from bovine blood; immunoglobulin γ (IGG) from human; insulin (INS) from bovine pancreas; lectin (LCL) from lentil; lipoxygenase-1 (LOX) from soybean; lysozyme (LSZ) from chicken egg white; myoglobin (MBN) from horse heart; monellin (MON) from *Dioscoreophyllum cumminsii*; metallothionein II (MTH) from rabbit liver; ovalbumin (OVA, egg albumin) from hen; parvalbumin (PAB) from rabbit muscle; penicillin amidohydrolase (PAH) from *Escherichia coli*; papain (PAP) from papaya latex; pepsin (PEP) from porcine stomach; peroxidase (PER) from *Arthromyces ramosus*; phosphoglyceric kinase (PGK) from *Saccharomyces cerevisiae*; pepsinogen (PGN) from pig stomach; phospholipase A2 (PLA) from bovine pancreas; R61 DD-transpeptidase from *Streptomyces r61*; rennin (REN, chymosin b) from calf stomach; ricin (RIC) from castor bean; ribonuclease A from bovine pancreas; subtilisin Carlsberg (SBC) from *Bacillus licheniformus*; subtilisin BPN′ (SBN, nagarse), source not specified; Fe-superoxide dismutase (SDF) from *E. coli*; Cu/Zn-superoxide dismutase (SOD) from bovine erythrocyte; trypsinogen (TGN) from bovine pancreas; trypsin inhibitor (TIB, Bowman-Burke inhibitor) from soybean; trypsin inhibitor (TIP, BPTI) from bovine pancreas; thaumatin (TMT) from *Thaumatococcus daniellii*; triose phosphate isomerase (TPI) from *S. cerevisiae*; troponin (TRO) from chicken muscle; ubiquitin (UBQ) from bovine erythrocyte; glucose oxidase (UOX) from *Aspergillus niger*; xylanase (XYN) from *Trichoderma viride*. See [18] for more details on the RASP50 FTIR database.

In addition to the RASP50 FTIR database spectra, a spectrum from the bacterial outer membrane protein OmpF porin reconstituted in asolectin phospholipid product (a gift from Dr F. Homblé, Université Libre de Bruxelles, Brussels, Belgium) and spectra of both Aβ-(1–42) fibrils and oligomers (see Figure 2) were used.

RESULTS

Aβ-(1–42) oligomers and fibrils: formation and assessments

Our goal in the present study was to compare the structure of Aβ-(1–42) oligomers and fibrils. We used established oligomer- or fibril-forming protocols to obtain the desired Aβ-(1–42) aggregates. Owing to the inherent high structural variability of the peptide, we carefully assessed each species using four independent approaches to verify that we obtained the expected entities.

Since Aβ-(1–42) is known to produce SDS-resistant oligomers and fibrils, we used Bis-Tris SDS/PAGE followed by 6E10 monoclonal antibody recognition to visualize the different species. After incubation at 4 °C for 24 h in TBS or F12, large oligomeric species appeared between ~40 and ~170 kDa (Figure 1A, lane 1). In acidic fibril-forming conditions, after 24 h of incubation, extremely-high-molecular-mass Aβ remained in the stacking gel. This high-molecular-mass Aβ corresponded to fibrils. A decrease of tri- and tetra-meric species was observed (Figure 1A, lane 2). With 7 days of incubation, in acidic fibril-forming conditions, the large oligomeric bands completely disappeared (Figure 1A, lane 3). Fibrils formed in 0.5 mM Hepes, pH 7.4, after 30 days also revealed an oligomer-free pattern (result not shown). It should be noted that the monomeric Aβ (~4.5 kDa) is present in all conditions. A quantification of the different band intensities using the ImageQuant TL software was carried out. It showed that in the oligomeric conditions (Figure 1A, lane 1), the band corresponding to the monomer represents only 16 % of the total intensity, whereas the larger oligomers (~40–170 kDa) represent 80 % (trimers and tetramers represent 2 % each). Such quantification is more difficult to perform for fibril-forming conditions because fibrils remain in the stacking gel and are probably underestimated. Nevertheless, this result demonstrates that monomers are clearly not the major species in our samples. As a comparison, with zero incubation ($t = 0$) in TBS, pH 7.4, Aβ-(1–42) forms small oligomers (mainly trimers and tetramers) in addition to monomers, which are the major species (~70 %). High-molecular-mass oligomers are also present on a $t = 0$ gel, but do not represent a significant proportion (~3 %) of the species formed by Aβ-(1–42) (results not shown).

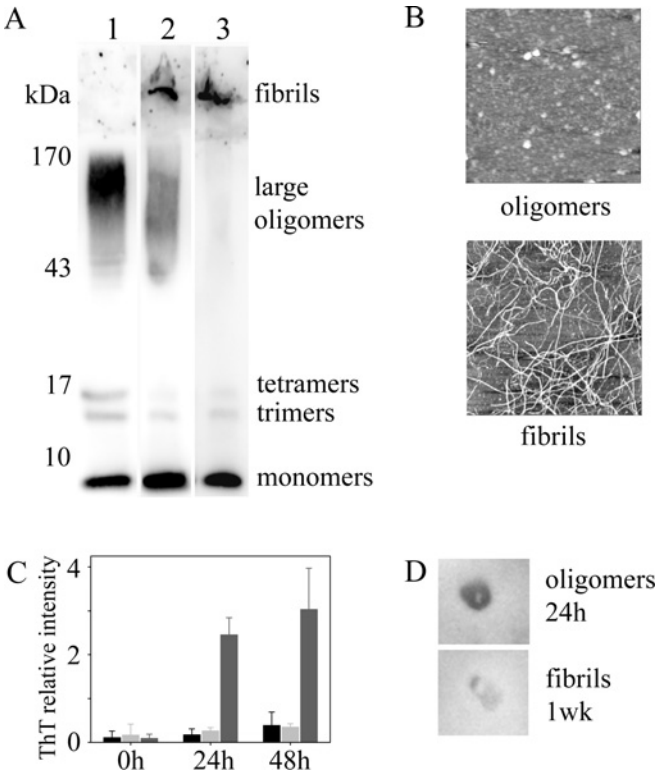

Figure 1 Assessments of Aβ-(1–42) under oligomer- and fibril-forming conditions

(**A**) Western blot analysis of Aβ-(1–42) oligomers and fibrils separated on a 12 % Bis-Tris SDS/PAGE gel and probed with the monoclonal antibody 6E10. Lane 1 shows Aβ-(1–42) oligomers formed in TBS after 24 h. Lanes 2 and 3 show Aβ-(1–42) fibrils formed in 10 mM HCl after 24 h and 7 days respectively. A quantification on non-overexposed blots has been carried out using the ImageQuant gel imager and software (see the text). Molecular masses are indicated in kDa. (**B**) AFM images of oligomeric and fibrillar Aβ-(1–42). AFM images were recorded in 2 μm × 2 μm contact mode with oligomers formed in TBS after 24 h (total *z* range = 15 nm) (upper panel) and 2 μm × 2 μm tapping mode with fibrils formed in 10 mM HCl after 24 h (total *z* range = 8 nm) (lower panel). (**C**) Relative ThT fluorescence emission intensity after 0, 24, and 48 h for Aβ-(1–42) oligomers formed in TBS (black), in F12 medium (light grey) and for Aβ-(1–42) fibrils formed in 10 mM HCl (dark grey). (**D**) Dot-blot analysis of 1 μg of Aβ-(1–42) oligomers formed in TBS after 24 h (upper panel) and fibrils formed in 10 mM HCl after 1 week (lower panel) with the conformation-dependent A11 antibody. The results shown here are representative of three to five independent experiments.

Even though Aβ is known to produce SDS-resistant oligomeric and/or fibrillar species, it has been shown that SDS/PAGE in the study of Aβ oligomers is not devoid of artefacts and might not always reflect the exact content of the different species present in the sample [6]. As suggested in [6], we undertook further characterization of both oligomers and fibrils to ensure that our samples were representative of each species.

A second method used to confirm fibril or oligomer formation was AFM. AFM images of oligomers formed after 24 h showed

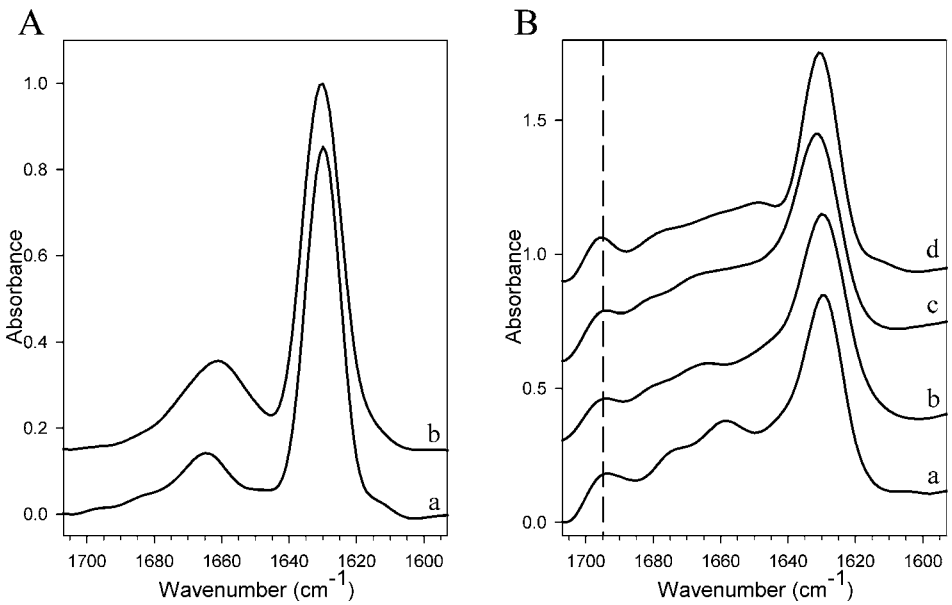

Figure 2 ATR-FTIR spectra in the amide I region of Aβ-(1–42) under fibril- and oligomer-forming conditions

(**A**) a, Aβ-(1–42) fibrils formed in 0.5 mM Hepes, pH 7.4, under agitation for 36 days. b, Aβ-(1–42) fibrils formed in 10 mM HCl during 7 days. (**B**) a and b, Aβ-(1–42) oligomers after incubation in TBS for <1 h and 24 h respectively. c, Aβ-(1–42) oligomers formed in F12 cell culture medium after 24 h. d, bacterial porin OmpF reconstituted in lipid membrane. A vertical broken line is shown at 1695 cm^{-1} to facilitate the identification of differences between spectra. Spectral intensities were normalized to the intensity of the 1630 cm^{-1} peaks. Spectra were shifted for better visualization. All spectra were deconvoluted using a Lorentzian deconvolution factor with a full width at half height of 20 cm^{-1}, a Gaussian apodization factor with a full width at half height of 13.33 cm^{-1} to obtain a resolution enhancement factor $K = 1.5$ [24]. Spectra are representative of at least three independent experiments.

the presence of globular spherical-shaped entities (Figure 1B, upper panel) with a typical height of 5–6 nm, which is in good agreement with previously characterized oligomers [19]. Importantly, it also showed that no fibrils were present in our oligomer-forming conditions. This verification was critical for the subsequent FTIR spectroscopic analysis, since it excluded potential spectral contributions from fibrils. In fibril-forming conditions, AFM images showed long unbranched fibrils with a typical 7–8 nm width (Figure 1B, lower panel). At higher magnification, these images showed some periodicity along the fibril axes (results not shown). All these features are in agreement with previously published data on Aβ fibrils [20]. To ensure that these fibrils were not formed during AFM sample preparation, especially during the removal of excess water at the mica plate, fibrillar samples were observed in contact-mode in buffer. These fibrillar samples were prepared in HCl and then resuspended in TBS, pH 7.4, to also ensure that a change in buffer and in pH did not affect the fibril morphology. The fibrils were not as well-resolved as in tapping-mode in air. However, the overall morphology and the size of the fibrils resembled those in tapping-mode (not shown), demonstrating that the removal of the excess water of the sample at the mica surface and a change in pH do not affect the fibrils once they are formed.

A third assessment was carried out using ThT fluorescence. ThT is known to fluoresce specifically in the presence of amyloid fibrils [16]. After resuspension ($t = 0$) of the Aβ-(1–42) peptide in all the conditions used in the present study, the samples were ThT negative. Both fibril-forming conditions resulted in a high ThT fluorescence emission intensity. This is already observed after 24 h for fibrils formed in 10 mM HCl. On the other hand, all of the oligomeric samples showed negligible ThT fluorescence emission intensity even after 48 h (Figure 1C).

Finally, using A11, an oligomeric conformation-specific antibody [12], we demonstrated using dot-blot analysis that oligomer-forming protocols yielded A11-positive results (Figure 1D, upper panel for oligomers formed in TBS). Fibrils formed in 10 mM HCl responded poorly or weakly to A11 after 1 week of incubation (Figure 1D, lower panel).

Taken together, these four experiments independently confirm that the oligomeric preparations: (i) do not have any fibrillar species; and (ii) do indeed contain moieties that are detected by the A11 antibody. Conversely, this analysis also ensures that our Aβ fibril samples are ThT-positive and devoid of oligomers. This rigorous pre-analysis is essential in our subsequent FTIR spectroscopic analysis to ensure that our oligomeric Aβ species do not contain any fibrillar species (and vice versa) that may potentially contribute to the spectral signals.

Secondary structure of oligomeric and fibrillar Aβ-(1–42) species

We next examined the secondary structure of these well-defined oligomeric and fibrillar Aβ-(1–42) species using ATR–FTIR spectroscopy. In FTIR spectroscopy, it has been demonstrated both theoretically and experimentally that parallel and antiparallel β-sheet structures can be distinguished based on the analysis of the amide I (1700–1600 cm^{-1}) region [21]. In antiparallel β-sheet structures, the amide I region displays two typical components. The major component has an average wavenumber located at $\sim$1630 cm^{-1}, whereas the minor component, approx. 5-fold weaker than the major one, is characterized by an average wavenumber at 1695 cm^{-1}. The 1695/1630 intensity ratio has been suggested to be proportional to the percentage of antiparallel arrangement of the β-strands in a β-sheet [22]. For parallel β-sheet structures, the amide I region displays only the major component around 1630 cm^{-1} [23,24].

FTIR spectra of Aβ-(1–42) in the two fibril-forming conditions employed in this study (Figure 2A, spectra a and b) showed typical parallel β-sheet features, characterized by a maximum of absorbance at 1630 cm^{-1} in the amide I region. The relatively narrow width of the major peak at 1630 cm^{-1} is indicative of

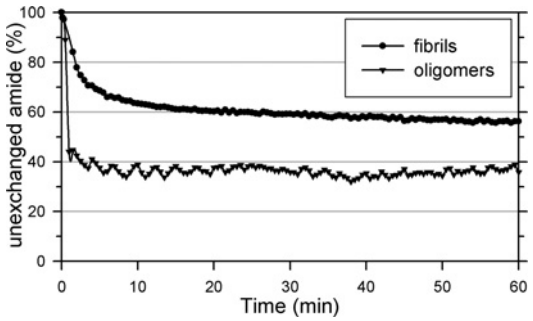

Figure 3 H–D exchange of Aβ-(1–42) fibrils and oligomers as a function of time

Fibrils were formed in 10 mM HCl and oligomers in TBS. Before experiments, the pH for both samples was adjusted to 6.5. Data are representative of at least three independent experiments, with S.D. $\leqslant$5 %.

stable and/or long β-strands and strong hydrogen bonds [24], as expected for extremely stable structures such as amyloid fibrils.

FTIR spectra of Aβ-(1–42) oligomers were significantly different from those of Aβ-(1–42) fibrils, indicating that these entities adopt a different structure. The amide I region is characterized by the presence of the two characteristic components of antiparallel β-sheet structure, at 1630 and 1695 cm^{-1} (Figure 2B, spectra a–c).

A quantitative analysis of the amide I region by deconvolution, followed by curve-fitting, showed that for both Aβ-(1–42) oligomers and fibrils, whereas β-sheet structures were the most abundant (48–57 % and ~75 % respectively), random coil and/or helical structures (observed absorbance around 1650–1660 cm^{-1}) represented ~20–26 and ~5–10 % for the oligomers and fibrils respectively. The helical content was slightly higher (33 and ~40 % if we take into account the random coil contribution) in oligomers incubated for less than 1 h, indicating a change in structure from α-helix to β-sheet with time. β-Turn content (~1670 cm^{-1}) was ~15–20 % for all the structures studied.

Solvent accessibility: H–D exchange experiments

To further analyse the structural difference between Aβ-(1–42) oligomers and fibrils, we performed H–D exchange experiments using FTIR spectroscopy. Whereas Aβ-(1–42) oligomers showed relatively fast exchange dynamics (approx. 60 % of amide hydrogens exchanged after 1 h), Aβ-(1–42) fibrils had slower exchange dynamics (only ~40 % of amide hydrogens exchanged during the same period of time) (Figure 3). The initial exchange rate was extremely high especially for oligomers, where most of the exchange occurred during the first 5 min.

Comparison with other proteins

In order to compare the different structures produced in the present study with known protein structures, we used a protein FTIR spectra database [18] designed to cover, as well as possible, the conformational space as defined by CATH (http://www.cathdb.info/) [25], with almost no redundancies. This database was previously shown to contain a number of unique features and allowed an improved structure prediction from IR spectra [26,27].

The overall shape of the Aβ-(1–42) spectra in the amide I and II range was compared with the entire database by means of a cluster analysis based on Euclidian distance measurement (see the Experimental section and Figure 4). The results demonstrated that: (i) Aβ fibrils spectra do not cluster with other protein spectra; and that (ii) Aβ oligomers spectra are clustered with five antiparallel β-sheet proteins (namely avidin, concanavalin A, lentil lectin, OmpF, and xylanase). From this cluster analysis, it is clear that OmpF spectrum is the closest and most related to the Aβ oligomer spectra (Figure 2B, spectrum d, and Figure 4). OmpF is folded as a typical antiparallel β-sheet barrel, made of 16 antiparallel strands, and is associated with an almost 100 % antiparallel arrangement of its β-strands [28]. The spectrum reveals the presence of 1630 and 1695 cm^{-1} peaks, attributed to antiparallel β-sheet structure. Using the respective 1695/1630 cm^{-1} intensity ratios [21] (Figure 5) for the different spectra displayed in Figure 2, we calculated that under all the oligomer-forming conditions used in the present study, the percentage of antiparallel arrangement of the β-strands was ~100 %, whereas under fibril-forming conditions this percentage was lower than 10 %.

DISCUSSION

The objective of the present study was to investigate the secondary structure adopted by oligomeric Aβ in comparison with fibrillar Aβ, in an effort to understand the structural basis of the neurotoxicity associated with the former. Although models for Aβ-(1–40) and Aβ-(1–42) in fibrillar conformations, mainly based on solid-state NMR data, are now accessible [29–32], almost no structural information for Aβ oligomers is currently available.

It is recognized that both species are characterized by the presence of β-sheet structures. However, fundamental differences in their local structures exist, conferring on them unique reactivity with conformation-specific antibodies. Using established conditions, we prepared Aβ-(1–42) oligomers and fibrils. The formation of Aβ oligomers or fibrils was confirmed with well-defined tests that mutually complement each other, such as: (i) the presence of SDS-resistant entities of multiple molecular masses by SDS/PAGE; (ii) visualization of oligomeric and fibrillar species by AFM; (iii) confirmation of the absence of fibrils in our oligomer preparations and of the presence of fibrils under our fibril-forming conditions by ThT fluorescence; and (iv) verification of the presence of A11-reactive species in our oligomer preparations, but not in our fibril preparations. This suite of assessments was critical for our subsequent FTIR spectroscopic analysis as it was important to demonstrate the absence of fibrillar Aβ in our oligomeric preparations and vice versa. As noted above, in the SDS/PAGE, one intriguing point is the presence of monomeric Aβ in each lane. This monomeric band, which is clearly not the most abundant entity (see the Results section), might be in part induced by the presence of SDS. If present in our samples, the monomers would contribute a constant spectral background in all our preparations.

After this initial confirmation, we employed ATR–FTIR spectroscopy to compare the structure of Aβ-(1–42) oligomers and fibrils. In fibrils, the presence of a major narrow peak located at ~1630 cm^{-1} was indicative of a highly stable parallel β-sheet, in agreement with solid-state NMR models [29–32] and site-directed spin labelling experiments [33], which showed that both Aβ-(1–40) and (1–42) adopt a cross-β structure with a parallel, in register (i.e. identical residues on adjacent chains are aligned), β-sheet composed of two strands connected by a turn or a loop region. Previously, 15–20 years ago, FTIR spectroscopy was misleading and demonstrated that Aβ fibrils adopted an antiparallel conformation. It is not the purpose of the present study to discuss why such a discrepancy occurred in the past. More recently, several groups have demonstrated that, for well-characterized parallel fibrils, the corresponding FTIR spectra were typical of parallel β-sheet {see examples in Figure 3d in

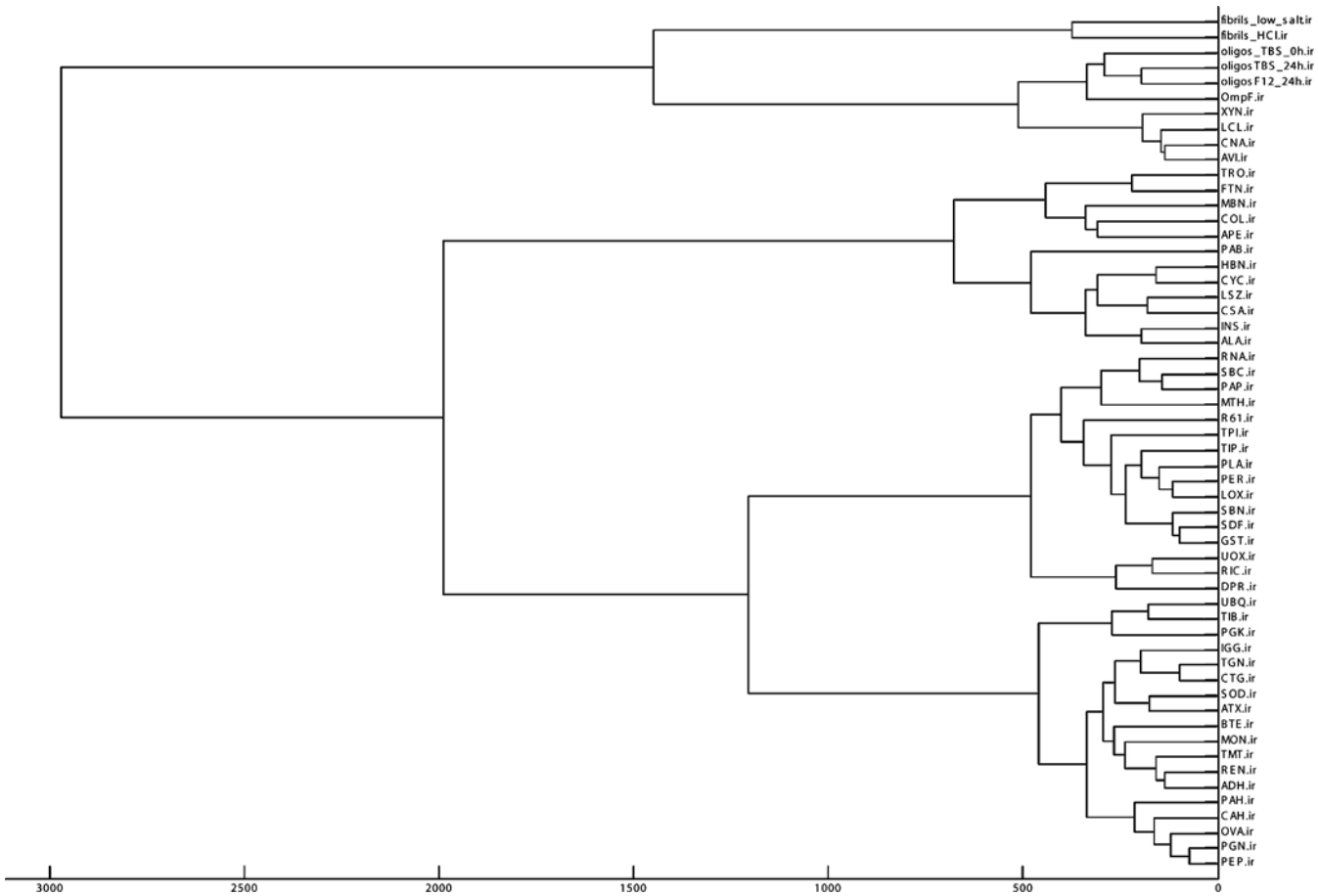

Figure 4 Dendrogram of the cluster analysis of RASP50, OmpF, Aβ-(1–42) fibril and oligomer spectra in the amide I and II range (1708–1482 cm^{-1})

Abscissa is the Euclidean distance (expressed in absorbance units) between spectra. On the ordinate the protein spectra identification are displayed. The proteins corresponding to the three letters code for RASP50 proteins are listed in the text. Ompf.ir corresponds to the FTIR spectrum of bacterial OmpF; fibrils_low_salt.ir corresponds to Aβ-(1–42) fibrils formed under low salt conditions; fibrils_HCl.ir corresponds to Aβ-(1–42) fibrils formed under acidic condition; oligos_TBS_0h.ir corresponds to Aβ-(1–42) oligomers formed in TBS ($t < 1$ h); oligosTBS_24h.ir corresponds to Aβ-(1–42) oligomers formed in TBS ($t = 24$ h); and oligosF12_24h.ir corresponds to Aβ-(1–42) formed in F12 cell culture medium ($t = 24$ h).

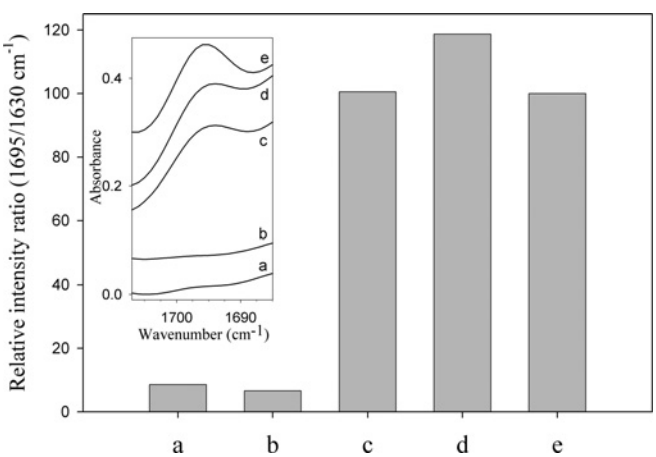

Figure 5 Relative intensity ratios of the 1695 and 1630 cm^{-1} peaks for Aβ-(1–42) fibrils and oligomers

a, Aβ-(1–42) fibrils formed in 0.5 mM Hepes, pH 7.4, under agitation for 30 days. b, Aβ-(1–42) fibrils formed in 10 mM HCl over 1 week. c, Aβ-(1–42) oligomers after incubation in TBS for 24 h. d, Aβ-(1–42) oligomers formed in F12 cell culture medium after 24 h. e, Bacterial porin OmpF reconstituted in lipid membrane. All of the 1695/1630 cm^{-1} ratios have been normalized on the OmpF ratio (taken as 100 %). Inset, corresponding FTIR spectra in the 1695 cm^{-1} region.

[34] for Aβ-(1–40) and Figure 2c in [35] for Aβ(1–28)}. On the contrary, for well-characterized antiparallel fibrils, FTIR spectra display two peaks (at $\sim$1630 and $\sim$1695 cm^{-1}) characteristic of antiparallel β-sheet (see examples in [36–38]).

A curve-fitting procedure of the IR spectra revealed that the β-sheet content in fibrils was as high as $\sim$75 %. Solvent accessibility evaluated by a NMR approach, indicated that there are two regions in Aβ-(1–42) fibrils protected from the solvent. These two regions encompass 70 % of the amino acids and are responsible for the formation of two strands in fibrils [39]. Using H–D exchange, we showed that $\sim$60 % of the amide bonds of the peptide were protected against the exchange in the fibril conformation, which is also in very good agreement with data provided by H–D exchange monitored by MS [40].

It is believed that, immediately upon its release from the membrane, Aβ oligomerizes in dimers and other multimers or soluble oligomers, and possibly forms fibrils. Also referred to as protofibrils or ADDLs, soluble oligomers mediate neuronal toxicity, inhibit long-term potentiation [41] and modulate neuronal viability [6,9], reflecting their inherent toxicity. Oligomers formed in F12 cell culture medium, using the same protocol as used in the present study, have been tested for their toxicity on Neuro-2A neuroblastoma cells [13]. The authors showed that Aβ-(1–42) oligomers inhibited neuronal viability 10-fold

more than Aβ-(1–42) fibrils. Using the same conditions, the same group has tested the toxicity of Aβ-(1–42) oligomers on neurons using primary co-cultures of neurons and glial cells [42]. They demonstrated that oligomeric Aβ-(1–42), but not fibrillar Aβ-(1–42), induced a dose-dependent increase in neurotoxicity. Thus the related toxicity of the Aβ-(1–42) oligomers we formed in the present study, has been carefully tested. Unfortunately little structural information is currently available on oligomers. Nevertheless, H–D exchange on Aβ-(1–40) protofibrils, which collectively referred to non-fibrillar oligomeric forms of Aβ, has shown that approx. 40 % of the amide backbone is highly resistant to exchange [40]. This is in excellent agreement with the percentage we determined in the present study on Aβ-(1–42) oligomers. This also establishes the validity of the approach we employed to assess the oligomeric species. The β-sheet content in oligomers was lower than in fibrils, but, however, was significant and reached 48–57 %. This lower content in secondary structure and faster exchange dynamics probably reflects a higher flexibility of Aβ in soluble oligomers than in fibrils. This higher flexibility (or lower stability) may be a crucial property of such assemblies, especially in their mechanism of toxicity. One of the hypothetical toxicity mechanisms for oligomers is related to their interaction with lipid bilayers in which they might cause perturbation and/or permeabilization [43–45].

Compared with fibrils, IR spectra of oligomers revealed the presence of an additional peak located at 1695 cm^{-1}, indicative of an antiparallel β-sheet conformation in these species. This additional peak has been recently observed in Aβ-(1–40) oligomers [34] and also in oligomers formed by a PrP (prion-related protein) peptide [PrP-(82–146)] [46]. This structural information suggests that even if fibrils and oligomers are rich in β-sheets, they do not adopt the same conformation. This is of significance in the neurotoxicity associated with oligomers. The antiparallel β-sheet organization in oligomers might represent a critical step in perturbation and/or permeabilization of biological membranes [43–45].

The A11 oligomer-specific antibody does not recognize fibrils, or low-molecular-mass oligomers, but is able to recognize the higher-molecular-mass prefibrillar oligomers of a wide variety of amyloidogenic peptides and proteins [12]. This suggests that most, if not all, amyloidogenic oligomers adopt the same structure and might share the same mechanism of toxicity. Recently, the same antibody was used with success against the pore-forming bacterial toxin, α-haemolysin, and on human perforin [47]. These proteins are known to form oligomeric pores in their toxic conformation, each monomer supplying several β-strands that self-assemble and fold into a β-barrel. It has been shown that Aβ and other amyloids can form annular or ring-shaped particles [44] which are comparable with pore-forming proteins.

IR spectra of Aβ oligomers presented striking similarities with bacterial outer membrane porins, which are folded as β-barrels. On the basis of the 1695/1630 cm^{-1} intensity ratios, we determined that Aβ oligomers were composed of β-strands, all of which were in an antiparallel organization. Interestingly, all pore-forming β-barrels adopt an antiparallel β-sheet organization. On the basis of the secondary structure content (45–50 % of extended β-sheet structures), we postulate a putative model wherein each Aβ molecule will provide two β-strands upon self-assembling during oligomer formation. In our view, the simplest way to accommodate two β-strands into the Aβ peptide in oligomeric conformation is to postulate that the two strands present in fibrils and approximately encompassing residues ~11–24 and ~28–42 [32], will form shorter β-strands in oligomers of approx. 10–12 residues each. These strands self-assemble in an antiparallel β-sheet conformation (Figures 2B, 4 and 6). Recently, the structure of monomeric Aβ-(1–40) in complex with a phage-display selected Affibody® protein has been solved by NMR spectroscopy [49]. This structure clearly showed that monomeric Aβ-(1–40) when stabilized by neighbour structural elements can adopt an antiparallel β-hairpin involving two β-strands encompassing residues 17–23 and 30–36. This is in good agreement with our proposed antiparallel β-sheet model. As suggested by Hoyer et al. [49], it can be speculated that, in our proposed model, a 'simple' reorientation of the plane of the strands by 90° will allow a reorganization from an antiparallel to a parallel β-sheet conformation, a conformational change that may be associated with the conversion from oligomeric to fibrillar Aβ and vice versa. Furthermore, it can be suggested that the antiparallel β-sheet conformation of oligomeric Aβ-(1–42) might, in some cases, be the early stages in the formation of a β-barrel made of 10–12 residue-long amphipathic strands. This β-barrel conformation (see Figure 6 for a schematic representation) is ideally suited to insert into a cellular membrane and span a lipid bilayer. Such an organization can potentially lead to permeabilization of cells, thereby contributing to the toxicity associated with these species. We suggest that, in the antiparallel conformation, the β-strands are organized in a manner that allows intramolecular hydrogen bond formation, and not only intermolecular ones like in fibrils.

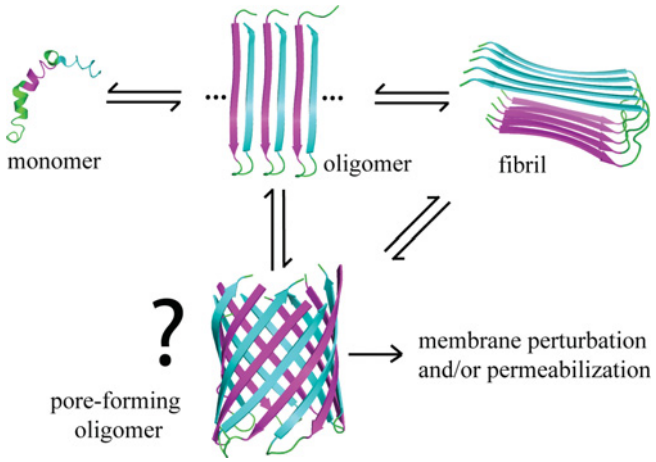

Figure 6 A hypothetical schematic representation of Aβ oligomers in a putative pore-forming conformation

The monomer structure of Aβ was taken from the 1Z0Q PDB file [48], fibril structure was derived from the 2BEG PDB file [29]. The size of the pore and the number of strands involved in pore formation are hypothetical. Residues involved in the central strand region are coloured magenta; those in the C-terminal portion of Aβ peptide are cyan. Non-structured regions are represented in green. The N-terminal region of the peptide is only represented in the monomer structure. The Figure was made using PyMOL (DeLano Scientific; http://www.pymol.org).

In conclusion, we demonstrated using ATR–FTIR spectroscopy that: (i) Aβ-(1–42) oligomers and fibrils can be clearly distinguished from each other and do not adopt the same secondary and tertiary structure; (ii) Aβ-(1–42) oligomers adopt an antiparallel β-sheet conformation and the antiparallel β-sheet structure may thus be a signature structural feature of oligomeric Aβ; and (iii) we showed some striking spectral similarities between Aβ oligomers and pore-forming porins and therefore believe that the ability of Aβ oligomers to form a porin-like structure may be associated with their toxicity in AD.

AUTHOR CONTRIBUTION

Emilie Cerf, Rabia Sarroukh and Vincent Raussens designed the research; Emilie Cerf, Rabia Sarroukh and Sylvie Derclaye performed the research; Emilie Cerf, Rabia Sarroukh,

Shiori Tamamizu-Kato, Leonid Breydo, Yves Dufrêne, Vasanthy Narayanaswami, Erik Goormaghtigh, Jean-Marie Ruysschaert and Vincent Raussens analysed data; and Emilie Cerf, Rabia Sarroukh, Vasanthy Narayanaswami, Erik Goormaghtigh, Jean-Marie Ruysschaert and Vincent Raussens wrote the paper.

ACKNOWLEDGMENTS

We thank Dr C. Govaerts and Dr F. Homblé for insightful discussions, Dr C. Glabe for kindly providing the A11 conformational-dependent antibody, Dr F. Homblé for providing the OmpF porin FTIR spectrum and Dr P. Boussard and Dr. Y. Looze for assistance and access to the fluorimeter.

FUNDING

E.C. is a Research Fellow for the National Fund for Scientific Research (Belgium); R.S. is Research Fellow for the Fund for Research in the Industry and Agriculture (Belgium); Y.F.D. and V.R. are Senior Research Associates; and E.G. is Research Director for the National Fund for Scientific Research (Belgium). V.N. was supported by funds from the Grant-In-Aid from the American Heart Association [grant number 0755137Y], the Drake Family trust and Tobacco-Related Disease Research Program [grant number 17RT-0165]. S.T.-K. is supported by a fellowship from the American Heart Association.

REFERENCES

1 Hardy, J. and Selkoe, D. J. (2002) The amyloid hypothesis of Alzheimer's disease: progress and problems on the road to therapeutics. Science **297**, 353–356
2 Selkoe, D. J. (1998) The cell biology of β-amyloid precursor protein and presenilin in Alzheimer's disease. Trends Cell Biol. **8**, 447–453
3 Vigo-Pelfrey, C., Lee, D., Keim, P., Lieberburg, I. and Schenk, D. B. (1993) Characterization of β-amyloid peptide from human cerebrospinal fluid. J. Neurochem. **61**, 1965–1968
4 Jarrett, J. T., Berger, E. P. and Lansbury, Jr, P. T. (1993) The carboxy terminus of the β amyloid protein is critical for the seeding of amyloid formation: implications for the pathogenesis of Alzheimer's disease. Biochemistry **32**, 4693–4697
5 Kim, W. and Hecht, M. H. (2005) Sequence determinants of enhanced amyloidogenicity of Alzheimer Aβ42 peptide relative to Aβ40. J. Biol. Chem. **280**, 35069–35076
6 Bitan, G., Fradinger, E. A., Spring, S. M. and Teplow, D. B. (2005) Neurotoxic protein oligomers: what you see is not always what you get. Amyloid **12**, 88–95
7 Kayed, R., Head, E., Sarsoza, F., Saing, T., Cotman, C. W., Necula, M., Margol, L., Wu, J., Breydo, L., Thompson, J. L. et al. (2007) Fibril specific, conformation dependent antibodies recognize a generic epitope common to amyloid fibrils and fibrillar oligomers that is absent in prefibrillar oligomers. Mol. Neurodegener. **2**, 18–28
8 Selkoe, D. J. (1996) Amyloid β-protein and the genetics of Alzheimer's disease. J. Biol. Chem. **271**, 18295–18298
9 Kirkitadze, M. D., Bitan, G. and Teplow, D. B. (2002) Paradigm shifts in Alzheimer's disease and other neurodegenerative disorders: the emerging role of oligomeric assemblies. J. Neurosci. Res. **69**, 567–577
10 Mucke, L., Masliah, E., Yu, G. Q., Mallory, M., Rockenstein, E. M., Tatsuno, G., Hu, K., Kholodenko, D., Johnson-Wood, K. and McConlogue, L. (2000) High-level neuronal expression of Aβ_{1-42} in wild-type human amyloid protein precursor transgenic mice: synaptotoxicity without plaque formation. J. Neurosci. **20**, 4050–4058
11 Necula, M., Kayed, R., Milton, S. and Glabe, C. G. (2007) Small molecule inhibitors of aggregation indicate that amyloid beta oligomerization and fibrillization pathways are independent and distinct. J. Biol. Chem. **282**, 10311–10324
12 Kayed, R., Head, E., Thompson, J. L., McIntire, T. M., Milton, S. C., Cotman, C. W. and Glabe, C. G. (2003) Common structure of soluble amyloid oligomers implies common mechanism of pathogenesis. Science **300**, 486–489
13 Dahlgren, K. N., Manelli, A. M., Stine, Jr, W. B., Baker, L. K., Krafft, G. A. and LaDu, M. J. (2002) Oligomeric and fibrillar species of amyloid-β peptides differentially affect neuronal viability. J. Biol. Chem. **277**, 32046–32053
14 Stine, Jr, W. B., Dahlgren, K. N., Krafft, G. A. and LaDu, M. J. (2003) *In vitro* characterization of conditions for amyloid-β peptide oligomerization and fibrillogenesis. J. Biol. Chem. **278**, 11612–11622
15 Garzon-Rodriguez, W., Sepulveda-Becerra, M., Milton, S. C. and Glabe, C. G. (1997) Soluble amyloid Aβ-(1–40) exists as a stable dimer at low concentrations. J. Biol. Chem. **272**, 21037–21044
16 LeVine, III, H. (1999) Quantification of β-sheet amyloid fibril structures with thioflavin T. Methods Enzymol. **309**, 274–284
17 Goormaghtigh, E., Raussens, V. and Ruysschaert, J.-M. (1999) Attenuated total reflection infrared spectroscopy of proteins and lipids in biological membranes. Biochim. Biophys. Acta **1422**, 105–185
18 Oberg, K. A., Ruysschaert, J. M. and Goormaghtigh, E. (2003) Rationally selected basis proteins: a new approach to selecting proteins for spectroscopic secondary structure analysis. Protein Sci. **12**, 2015–2031
19 Mastrangelo, I. A., Ahmed, M., Sato, T., Liu, W., Wang, C., Hough, P. and Smith, S. O. (2006) High-resolution atomic force microscopy of soluble Aβ42 oligomers. J. Mol. Biol. **358**, 106–119
20 Stromer, T. and Serpell, L. C. (2005) Structure and morphology of the Alzheimer's amyloid fibril. Microsc. Res. Tech. **67**, 210–217
21 Miyazawa, T. and Blout, E. R. (1961) The infrared spectra of polypeptides in various conformations: amide I and amide II bands. J. Am. Chem. Soc. **83**, 712–719
22 Chirgadze, Y. N. and Nevskaya, N. A. (1976) Infrared spectra and resonance interaction of amide-I vibration of the antiparallel-chain pleated sheet. Biopolymers **15**, 607–625
23 Chirgadze, Y. N. and Nevskaya, N. A. (1976) Infrared spectra and resonance interaction of amide-I vibration of the parallel-chain pleated sheet. Biopolymers **15**, 627–636
24 Goormaghtigh, E., Cabiaux, V. and Ruysschaert, J.-M. (1994) Determination of soluble and membrane protein structure by Fourier transform infrared spectroscopy. I. Assignments and model compounds. Subcell. Biochem. **23**, 329–362
25 Orengo, C. A., Michie, A. D., Jones, S., Jones, D. T., Swindells, M. B. and Thornton, J. M. (1997) CATH: a hierarchic classification of protein domain structures. Structure **5**, 1093–1108
26 Oberg, K. A., Ruysschaert, J.-M. and Goormaghtigh, E. (2004) The optimization of protein secondary structure determination with infrared and circular dichroism spectra. Eur. J. Biochem. **271**, 2937–2948
27 Goormaghtigh, E., Ruysschaert, J.-M. and Raussens, V. (2006) Evaluation of the information content in infrared spectra for protein secondary structure determination. Biophys. J. **90**, 2946–2957
28 Cowan, S. W., Schirmer, T., Rummel, G., Steiert, M., Ghosh, R., Pauptit, R. A., Jansonius, J. N. and Rosenbusch, J. P. (1992) Crystal structures explain functional properties of two E. coli porins. Nature **358**, 727–733
29 Antzutkin, O. N., Balbach, J. J., Leapman, R. D., Rizzo, N. W., Reed, J. and Tycko, R. (2000) Multiple quantum solid-state NMR indicates a parallel, not antiparallel, organization of beta-sheets in Alzheimer's β-amyloid fibrils. Proc. Natl. Acad. Sci. U.S.A. **97**, 13045–13050
30 Petkova, A. T., Ishii, Y., Balbach, J. J., Antzutkin, O. N., Leapman, R. D., Delaglio, F. and Tycko, R. (2002) A structural model for Alzheimer's β-amyloid fibrils based on experimental constraints from solid state NMR. Proc. Natl. Acad. Sci. U.S.A. **99**, 16742–16747
31 Petkova, A. T., Yau, W-M. and Tycko, R. (2006) Experimental constraints on quaternary structure in Alzheimer's beta-amyloid fibrils. Biochemistry **45**, 498–512
32 Lührs, T., Ritter, C., Adrian, M., Riek-Loher, D., Bohrmann, B., Döbeli, H., Schubert, D. and Riek, R. (2005) 3D structure of Alzheimer's amyloid-β(1–42) fibrils. Proc. Natl. Acad. Sci. U.S.A. **102**, 17342–17347
33 Török, M., Milton, S., Kayed, R., Wu, P., McIntire, T., Glabe, C. G. and Langen, R. (2002) Structural and dynamic features of Alzheimer's Aβ peptide in amyloid fibrils studied by site-directed spin labeling. J. Biol. Chem. **277**, 40810–40815
34 Habicht, G., Haupt, C., Friedrich, R. P., Horstchansky, P., Sachse, C., Meinhardt, J., Wieligmann, K., Gellerman, G.P., Brodhun, M., Götz, J., et al. (2007) Directed selection of a conformational antibody domain that prevents mature amyloid fibril formation by stabilizing Aβ protofibrils. Proc. Natl. Acad. Sci. U.S.A. **104**, 19232–19237
35 Perálvarez-Marín, A., Barth, A. and Gräslund, A. (2008) Time-resolved infrared spectroscopy of pH-induced aggregation of the Alzheimer Aβ_{1-28} peptide. J. Mol. Biol. **379**, 589–596
36 Dzwolak, W. and Smirnovas, V. (2005) A conformational α-helix to β-sheet transition accompanies racemic self-assembly of polylysine: an FT-IR spectroscopic study. Biophys. Chem. **115**, 49–54
37 Castelletto, V., Hamley, I. W. and Harris, P. J. F. (2008) Self-assembly in aqueous solution of a modified amyloid β peptide fragment. Biophys. Chem. **138**, 29–35
38 Lee, S.-W., Mou, Y., Lin, S.-Y., Chou, F.-C., Tseng, W. H., Chen, C.-H., Lu, C.-Y.D., Yu, S. S.-F. and Chan, J. C. C. (2008) Steric zipper of the amyloid fibrils formed by residues 109–122 of the Syrian hamster prion protein. J. Mol. Biol. **378**, 1142–1154
39 Olofsson, A., Sauer-Eriksson, A. E. and Öhman, A. (2006) The solvent protection of Alzheimer amyloid-β-(1–42) fibrils as determined by solution NMR spectroscopy. J. Biol. Chem. **281**, 477–483
40 Kheterpal, I., Lashuel, H. A., Hartley, D. M., Waltz, T., Lansbury, P. T. and Wetzel, R. (2003) Aβ protofibrils possess a stable core structure resistant to hydrogen exchange. Biochemistry **42**, 14092–14098

41 Walsh, D. M., Klyubin, I., Fadeeva, J. V., Cullen, W. K., Anwyl, R., Wolfe, M. S., Rowan, M. J. and Selkoe, D. J. (2002) Naturally secreted oligomers of amyloid beta protein potently inhibit hippocampal long-term potentiation *in vivo*. Nature **416**, 535–539
42 Manelli, A. M., Bulfinch, L. C., Sullivan, P. M. and LaDu, M. J. (2007) Aβ42 neurotoxicity in primary co-cultures: effect of apoE isoform and Aβ conformation. Neurobiol. Aging **28**, 1139–1147
43 Kayed, R., Sokolov, Y., Edmonds, B., McIntire, T. M., Milton, S. C., Hall, J. E. and Glabe, C. G. (2004) Permeabilization of lipid bilayers is a common conformation-dependent activity of soluble amyloid oligomers in protein misfolding diseases. J. Biol. Chem. **279**, 46363–46366
44 Lashuel, H. A., Hartley, D., Petre, B. M., Walz, T. and Lansbury, Jr., P. T. (2002) Neurodegenerative disease: amyloid pores from pathogenic mutations. Nature **418**, 291
45 Kremer, J. J., Pallitto, M. M., Sklansky, D. J. and Murphy, R. M. (2000) Correlation of β-amyloid aggregate size and hydrophobicity with decreased bilayer fluidity of model membranes. Biochemistry **39**, 10309–10318
46 Natalello, A., Prokorov, V. V., Tagliavini, F., Morbin, M., Forloni, G., Beeg, M., Manzoni, C., Colombo, L., Gobbi, M., Salmona, M. and Doglia, S. M. (2008) Conformational plasticity of the Gerstmann-Sträussler-Scheinker disease peptide as indicated by its multiple aggregation pathways. J. Mol. Biol. **381**, 1349–1361
47 Yoshiike, Y., Kayed, R., Milton, S. C., Takashima, A. and Glabe, C. G. (2007) Pore-forming proteins share structural and functional homology with amyloid oligomers. Neuromol. Med. **9**, 270–275
48 Tomaselli, S., Esposito, V., Vangone, P., van Nuland, N. A., Bonvin, A. M., Guerrini, R., Tancredi, T., Temussi, P. A. and Picone, D. (2006) The α-to-β conformational transition of Alzheimer's Aβ-(1–42) peptide in aqueous media is reversible: a step by step conformational analysis suggests the location of beta conformation seeding. Chembiochem **7**, 257–267
49 Hoyer, W., Grönwall, C., Jonsson, A., Ståhl, S. and Härd, T. (2008) Stabilization of a β-hairpin in monomeric Alzheimer's amyloid-β peptide inhibits amyloid formation. Proc. Natl. Acad. Sci. U.S.A. **105**, 5099–5104

Received 4 March 2009/6 May 2009; accepted 13 May 2009
Published as BJ Immediate Publication 13 May 2009, doi:10.1042/BJ20090379